

other molecular tools⁶. In the present study, we have successfully demonstrated the superiority of qRT-PCR over RT-PCR by detecting CHIKV-RNA in dead mosquitoes and serum samples stored at higher temperatures for longer period. QRT-PCR could find application in diagnosis of CHIKV during outbreaks as well as field based surveillance of CHIKV in mosquitoes/blood samples. This will be a boon for resource constraint countries where cold chain maintenance is a concern. Our findings have strongly shown that CHIKV remained viable for a substantial period of time even at 37°C in blood samples posing a threat to clinicians and laboratory personnel who handle patients and clinical samples.

Conflict of interest: The authors declare that they have no conflict of interest.

1. Peterson, L. R. and Powers, A. M., *Chikungunya: epidemiology*. F1000Res (2016); 5. pii: F1000 Faculty Rev-82. doi:10.12688/f1000research.7171.1.eCollection 2016.
2. Ramachandrarao, T., Sharda Devi, P. and Singh, K. R., *Mosq. News*, 1968, **28**, 406–408.

3. Sudeep, A. B., Ghodke, Y. S., Gokhale, M. D., George, R. P., Dhaigude, S. D. and Bondre, V. P., *J. Vector Borne Dis.*, 2014, **51**, 333–338.
4. Reed, L. J. and Muench, H. A., *Am. J. Hyg.*, 1938, **27**, 493–497.
5. Parashar, D., Amdekar, S., More, A., More, R., Patil, P. and Ravindra Babu, V., *Indian J. Med. Res. (Supplement)*, 2015, **142**, 62–66.
6. Parashar, D., Paingankar, M. S., Sudeep, A. B., More, A., Shinde, S. and Arankalle, V. A., *Curr. Sci.*, 2014, **107**, 211–213.
7. Parashar, D., Paingankar, M. S., Kumar, S., Gokhale, M. D., Sudeep, A. B., Shinde, S. B. and Arankalle, V. A., *PLoS Negl. Trop. Dis.*, 2013, **7**, e2405.
8. Mavale, M. *et al.*, *Am. J. Trop. Med. Hyg.*, 2012, **86**, 178–180.
9. Damjanovic, V., *J. Hosp. Infect.*, 1987, **10**, 209–211.
10. Dimmock, N. J., *Virology*, 1967, **31**, 338–353.
11. Salvucci, J. T., *Cell Tissue Bank*, 2011, **12**, 99–104.
12. Bean, B., Moore, B. M., Sterner, B., Peterson, L. R., Gerding, D. N. and Balfour Jr, H. H., *J. Infect. Dis.*, 1982, **146**, 47–51.
13. Sebire, K., McGavin, K., Land, S., Middleton, T. and Birch, C., *J. Clin. Microbiol.*, 1998, **36**, 493–498.
14. Tjotta, E., Hungnes, O. and Grinde, B., *J. Med. Virol.*, 1991, **35**, 223–227.
15. Painsil, E., Binka, M., Patel, A., Lindenschmidt, B. D. and Heimer, R., *J. Infect. Dis.*, 2014, **209**, 1205–1211.
16. Detmer, J. *et al.*, *J. Clin. Microbiol.*, 1996, **34**, 901–907.

ACKNOWLEDGEMENTS. The authors acknowledge financial support provided by the Indian Council of Medical Research, Ministry of Health and Family Welfare, Government of India.

Received 29 January 2018; revised accepted 20 April 2018

DEEPTI PARASHAR*
A. B. SUDEEP
ASHWINI MORE
POONAM PATIL
ATUL WALIMBE
MANGALA MAVALE
SARIKA AMDEKAR

*ICMR-National Institute of Virology,
20A, Ambedkar Road,
Pune 411 001, India*

**For correspondence.
e-mail: deeptiparasharster@gmail.com*

Total electron content and epicentral distance of 2015 M_w 7.8 Nepal earthquake revealed by continuous observations data

A large magnitude (M_w 7.8) earthquake occurred on 25 April 2015 (06:11 UTC) at 28.1473°N and 84.7079°E, 34 km east-southeast of Lamjung, Nepal. The devastating event was accompanied by two large aftershocks of M_w 6.6 (on 25 April 2015, 06:45 UTC) and M_w 6.7 (on 26 April 2015 at 09:10 UTC). According to the USGS earthquake catalogue, 65 aftershocks were recorded within a period of three days from the main event; the strongest aftershock had occurred on 12 May 2015 at 07:05 UTC.

Here we report the ionosphere total electron content (TEC) anomaly prior to the main shock on 25 April 2015, observed from the data of 14 Global Navigation Satellite System (GNSS) stations (plate boundary observatories) at Nepal maintained by UNAVCO, USA. Ionosphere TEC and its deviation from the average concentration have been studied

for a number of earthquakes worldwide using GNSS data. These studies are limited to statistical analysis for TEC variations prior to events from GNSS observations close to the epicentre, or at least falling within the earthquake preparatory zone^{1,2}. In this study, data from 14 continuously operating stations were used in the estimation of vertical TEC using the program GPS-TEC^{3–5}. Time-series analysis of TEC for a period of 30 days was carried out and anomalies were detected using 15 days running average plus/minus two times 15 days running standard deviation. The TEC values crossing these limits were considered as anomalies. The TEC values corresponding to the anomaly time for all 14 stations were detected and interpolated to plot in two-dimensions to observe the TEC spatial pattern (Figure 1).

The link between ionospheric TEC anomalies and earthquake occurrences has been reported in many studies. This is basically governed by the lithosphere–atmosphere–ionosphere coupling mechanism. The ionosphere records the earthquake due to change in global electric circuit produced by the cluster of ions in the atmosphere emanating due to the development of stress in the crustal region prior to an earthquake^{6,7}.

The TEC time-series analysis was carried out using GNSS observation stations located at 30–300 km areal distance from the epicentre of the 2015 M_w 7.8 Gorkha earthquake. Analysis with 15 days mean ± 2 standard deviation limit, reveals negative (low) TEC anomaly on 11 April 2015, whereas positive (high) anomaly on 24 April 2015 was measured at station BESI (Besihari, Lumjung) located at 30 km distance from the

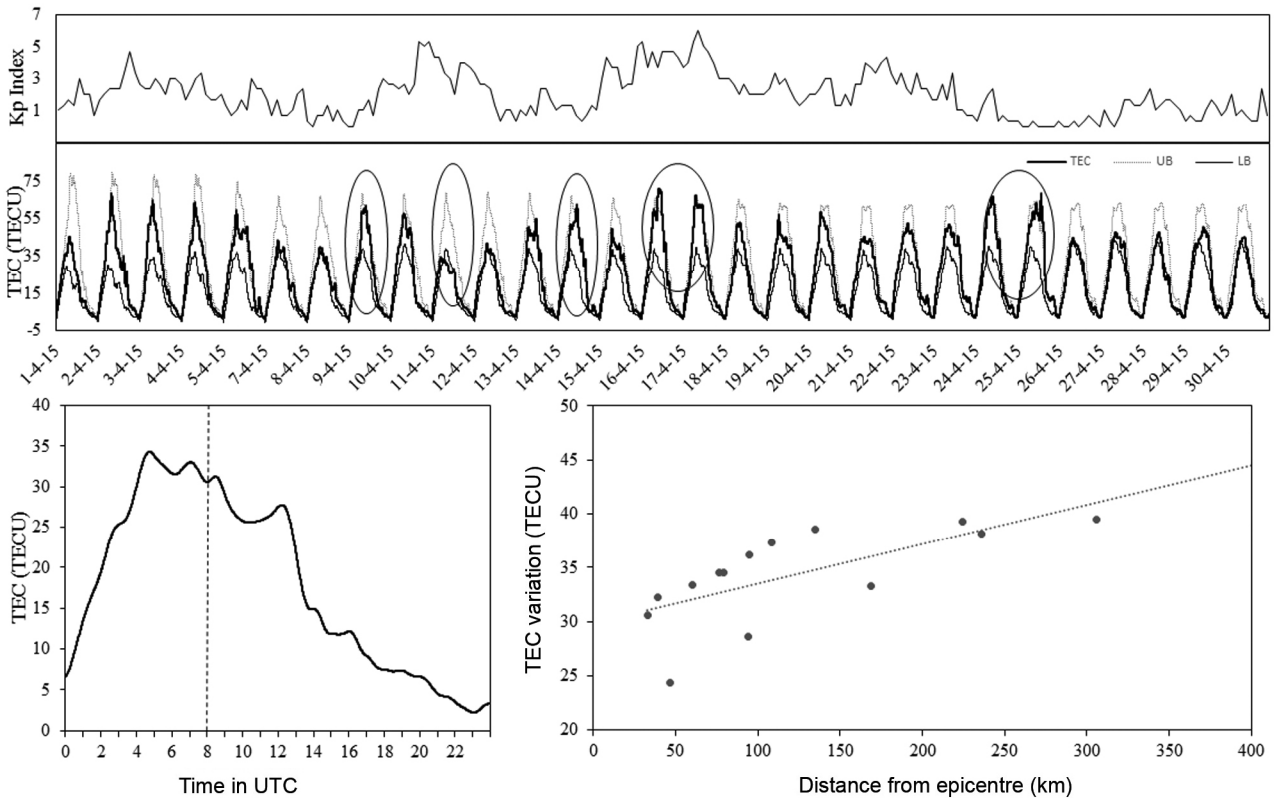


Figure 1. TEC time series plot, geomagnetic storm index, TEC anomaly time, and TEC distribution for 14 GNSS stations. (Middle) TEC time series for 30 days at Besihari, Lumjung (BESI) 30 km from the epicentre. (Top) Geomagnetic storm index (K_p index) for a period of 30 days vis-à-vis TEC variation. K_p index on 17 April 2015 ($K_p = 6$) reveals minor storm activity. (Bottom, left) TEC fluctuation on 11 April 2015 at BESI (Besihari, Nepal). Dashed line represents TEC anomaly time: 8:00 UTC. (Bottom) TEC values corresponding to 14 GNSS stations at Nepal, detected during the anomaly time (08:00 UTC)

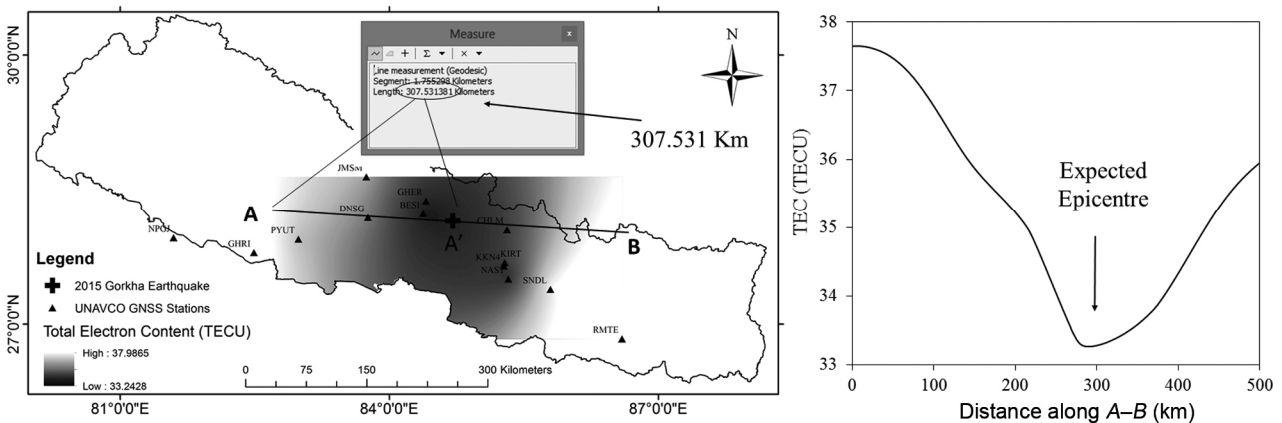


Figure 2. Relationship between TEC and distance from the epicentre. (Left) Spatial distribution of TEC values for 14 stations at the detected anomaly time (08:00 UTC) on 11 April 2015. (Right) Profile along AB. The low TEC zone is the expected epicentre region at around 300 km from A and it coincides well with the actual epicentre (A') of the earthquake on 25 April 2015.

epicentre. Additionally, positive anomalies were also observed on 9, 14, 16, 17 and 25 April 2015.

The space weather conditions were considered to rule out their influence and finally it was confirmed that the detected anomalies were seismicogenic in nature.

Minor geomagnetic storm for short duration was observed on 17 April 2015 and hence the increase in TEC could be due to this activity on that day. Various indices are used for the assessment of geomagnetic storm activities. We have used K_p index provided by the National Oceanic and Atmospheric Administration (NOAA), US Department of Commerce for assessing geomagnetic activities (Figure 1). A K_p index of 6 was observed on 17 April 2015, suggesting geomagnetic storm activity of low intensity. The exact anomaly times were detected for 11

anic and Atmospheric Administration (NOAA), US Department of Commerce for assessing geomagnetic activities (Figure 1). A K_p index of 6 was observed on 17 April 2015, suggesting geomagnetic storm activity of low intensity. The exact anomaly times were detected for 11

and 24 April and were found to be 8 and 9 UTC respectively. The TEC values corresponding to the anomaly time for all 14 stations (locations) suggest that the TEC gradient decreased towards the epicentre on 11 April when negative anomaly was observed, and increased towards the epicentre on 24 April when positive anomaly was observed. This opens a new avenue for possible detection of the epicentre by establishing a large number of ground networks of GNSS. Figures 1 and 2 show TEC changes on 11 April 2015 at 8 UTC from 14 GNSS stations in Nepal. The TEC profile along *AB* shows a reduction of TEC at a distance of around 300 km from *A*, which could be the expected epicentre (Figure 2). When measured along *A* and the actual epicentre *A'*, the distance between them is found to be 307.5 km. Therefore, there is a definite pattern showing decreased TEC gradient towards the epicentre, where a negative anomaly is observed. This information can help in detecting the epicentre of impending earthquakes from a large number of GNSS observations. Thus, continuous ionospheric TEC monitoring with well-distributed GNSS observation stations may open up a new avenue

towards precursor monitoring and epicentre detection of impending earthquakes.

1. Liu, J. Y., Chuo, Y. J., Shan, S. J., Tsai, Y. B., Chen, Y. I., Pulinet, S. A. and Yu, S. B., *Ann. Geophys.*, 2004, **22**, 1585–1593.
2. Sharma, G., Champatiray, P. K., Mohanty S. and Kannaujiya, S., *Quaternary Int.*, 2017, **462**, 65–74.
3. Abba, I., Abidin, W. A. W. Z., Masri, T., Ping, K. H., Muhammad, M. S. and Pai, B. V., *Niger. J. Technol.*, 2015, **34**(3), 523–529.
4. Ndeda, J. O. H. and Odera, P. O., *Appl. Phys. Res.*, 2014, **6**(1), 19–25.
5. Adewale, A. O., Oyeyemi, E. O., Adeniyi, J. O., Adeloye, A. B. and Oladipo, O. A., *Indian J. Radio Space Phys.*, 2011, **40**, 21–25.
6. Pulinet, S. A., *Terrestrial Atm. Oceanic Sci.*, 2004, **15**(3), 413–435.
7. Friedemann, F. T., Kulahci, I., Cyr, G., Ling, J., Winnick, M., Tregloan-Reed, J., and Freund, M. M., *J. Atmos. Solar-Terrestrial Phys.*, 2009, **71**, 1824–1834.

ACKNOWLEDGEMENTS. We thank UNAVCO, USA, formerly called University NAVSTAR Consortium for providing high-quality GNSS data free of cost for analysis

and Dr Gopi Seemala (Indian Institute of Geomagnetism, Mumbai) for providing the latest version of GPSTEC software for TEC computation. We also thank the International GNSS Services (IGS) and National Oceanic and Atmospheric Administration (NOAA), US Department of Commerce for providing derived product and correction parameter files for the present analysis.

Received 5 November 2017; accepted 3 May 2018

GOPAL SHARMA^{1,*}
S. MOHANTY²
P. K. CHAMPATI RAY³
M. SOMORJIT SINGH¹
K. K. SARMA¹
P. L. N. RAJU¹

¹North Eastern Space Application
Centre,

Umiam 793 103, India

²Indian Institute of Technology
(Indian School of Mines),

Dhanbad 826 004, India

³Indian Institute of Remote Sensing,
Dehradun 248 001, India

*For correspondence.

e-mail: gops.geo@gmail.com

Invasion and establishment of the solanum whitefly *Aleurothrixus trachoides* (Back) (Hemiptera: Aleyrodidae) in South India

Trade, transport and travel are the major drivers of bioinvasions and will continue to increase as a by-product of globalization¹. Agricultural practices that simplify ecosystems by focusing on a small number of crops by eliminating predators and competitors generally make those systems more vulnerable to invasion². The Neotropical solanum whitefly, *Aleurothrixus trachoides* is found to be invasive in India³; it is presently spreading fast in South India infesting many economically important plants of the family Solanaceae like brinjal (Figure 1 a), chilli (Figure 1 b), and tomato (Figure 1 c), and sandalwood (Figure 1 d), as well as some medicinal, ornamental (Figure 1 e) and weed species (Figure 1 f).

Whiteflies comprise the insect family Aleyrodidae and are an economically important group of small inconspicuous

phytophagous insects; they are often overlooked despite their abundance on the surfaces of leaves⁴. Whiteflies rank among the most noxious insects attacking field crops and greenhouse crops around the world. The economic loss is due to their activities of sucking the plant sap, acting as vectors of viral diseases and in production of honey dew leading to the development of mould on leaves, thus adversely affecting photosynthesis⁵. So far 440 species of whiteflies under 63 genera are known from India, among which few are economically important.

Whiteflies pose a significant threat to agriculturists throughout the world. Globally over the past 25 years, exotic whiteflies have invaded several countries causing direct losses in agriculture, horticulture and forestry. A news report on 'Whiteflies destroying two-thirds of Punjab's cotton crop, resulting in 15 farmer

suicides' (*Times of India*, 8 October 2015) is one such example in India. The spiralling whitefly *Aleurodicus disperses* invaded India in 1995 (ref. 6) and its spread was successful mainly due to its polyphagous nature and prolific breeding. Impact of its infestation on Indian agricultural economy is well recognized as it affects many economically important plants. The whitefly is breeding on over 320 plant species belonging to 225 genera and 73 families in India⁷. However, now its management is possible due to extensive research coupled with introduction of exotic parasitoids. The agricultural economy in India is vulnerable to the emerging threat by invasion of the solanum whitefly as brinjal, chilli, tomato, etc. are important solanaceous fruit vegetables grown in our country.

A. trachoides is a native of the Neotropical Region, but had become